Planar-lens Enabled Beam Steering for Chip-scale LIDAR

Josué J. López[1], Scott A. Skirlo[1], Dave Kharas[2], Jamison Sloan[1], Jeffrey Herd[2], Paul Juodawlkis[2], Marin Soljačić[1], Cheryl Sorace-Agaskar[2]

[1]*Massachusetts Institute of Technology, Cambridge MA 02139, USA*
[2]*MIT Lincoln Laboratory, Lexington, MA 02421, USA*

jjlopez@mit.edu, scott.skirlo.3@us.af.mil

Abstract: A lens-enabled chip-scale beam steering device for LIDAR is theoretically analyzed and experimentally demonstrated with azimuthal, ϕ_{range} = 38.8°, and polar, θ_{range} = 12.0°, beam-steering. The device allows for beam-steering at low power and low cost.

OCIS codes: (130.3120) Integrated optics devices; (250.5300) Photonic integrated circuits; (280.3640) LIDAR

Light Detection and Ranging (LIDAR) has attracted significant interest in a variety of application spaces including autonomous navigation. In particular, there is demand for a compact, non-mechanically steered sensor. Several candidate technologies are being explored, including micro-mechanical mirrors, liquid-crystal based devices, and integrated photonics. The current leading chip-based LIDAR uses 1D or 2D phased array antennas to steer a coherent beam bidirectionally [1, 2]. In many ways, phased array LIDAR is the photonic counterpart of RF phased array radar which was originally challenging as well. Interestingly, the radar literature contains a class of planar-lens based beam steering solutions (e.g. Rotman lenses) that overcame challenges in the RF domain to produce wider-angle scanning, narrower beams, and higher beam quality [3]. Their integrated-photonic analogs have not yet been investigated and are a viable solution for chip-scale optical LIDAR. Herein, for the first time, we explore this new class of devices through a comparison of theory, simulations, and experimentally prototyped photonic integrated circuits (PICs).

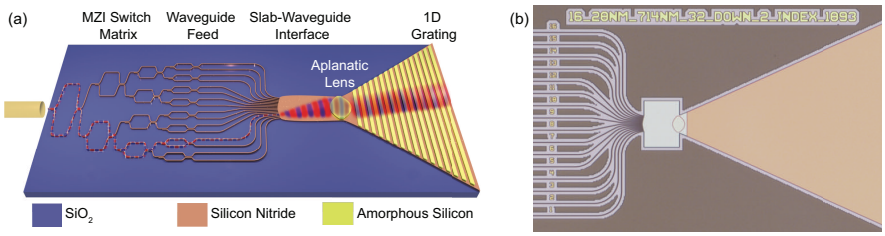

Fig. 1: (a) Proposed integrated system: An IR signal λ=(1500-1600 nm) is coupled into the chip. The signal is routed through an optical switch matrix formed by an array of Mach-Zehnder switches. The IR beam is then emitted into the focal plane of the lens, undergoing diffraction until being focused by the planar lens. It is then scattered out-of-plane by a 1D grating coupler. (b) Optical microscope image of fabricated waveguide array input to beam-steering lens and grating coupler.

A schematic of this lens-based beam-steering device is seen in Fig. 1. First, a tunable IR source centered at λ_0=1.55 μm is fiber-coupled to an on-chip, silicon nitride (SiN) waveguide. Next the signal is routed through a switch matrix composed of a depth tree of Mach-Zehnder interferometric switches (of size N) which use integrated thermo-optic (TO) phase shifters. Then, light from the waveguide enters a slab waveguide, where it is diffracted and then refocused by an aplanatic lens, formed from a patterned amorphous silicon (a-Si) layer. Finally, the collimated beam propagates into a 1D grating where it is scattered out-of-plane.

Beam steering for the chip is achieved through two mechanisms. (1) Port switching changes the in-plane angle of propagation into the lens and consequently the azimuthal angle, ϕ, enabling wide-angle steering, as seen in Fig. 2a. (2) Wavelength (λ) tuning changes the polar angle, θ, at which the collimated beam is scattered out of the grating and into the far-field. Given a 1D grating, switching ports translates the emitted beam along an elliptical arc defined by $((u_{x,0} + \frac{m\lambda}{\Lambda})/n_{\text{eff}})^2 + (u_{y,0}/n_1)^2 = 1$. Where $u_{x,0} = \sin(\psi_0)\cos(\theta_0)$ and $u_{y,0} = \sin(\psi_0)\sin(\theta_0)$, ψ_0 is the angle in the plane of the chip, m is the grating order, λ is the laser wavelength, Λ is the grating period, n_{eff} is the effective index of the grating, and n_1 is the effective index of the TE slab mode. Tuning λ translates this arc up and down, Fig. 2b-c.

This architecture has several advantages over traditional phased-array approaches. First, because only a sub-set of the switches are used simultaneously, the phase-shifter power requirements scale as $\log_2 N$, where N is the number of ports, whereas phased-array architectures scale with N, where N is the number of antenna elements. This can lead to large power savings when a large number of far-field spots are desired. Second, this approach avoids the phasing

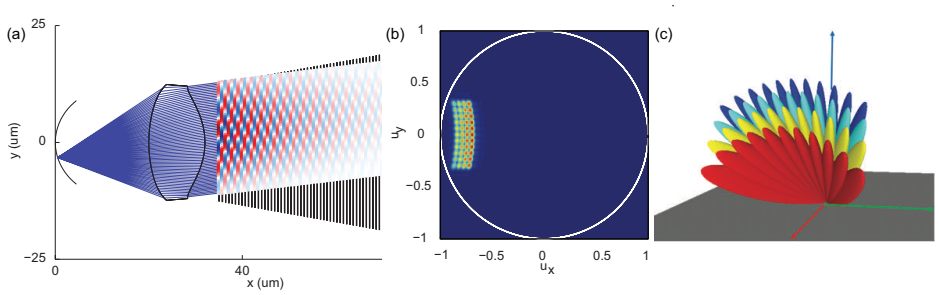

Fig. 2: (a) Theoretical ray-tracing is used to determine optimal port position and angle into the grating. (b) Heat plot showing far-field beam spots in u_x and u_y space. Movement along the elliptical curve happens via port switching. Translating the curve right and left corresponds to λ_0 tuning. (c) 3D beam patterns corresponding to those in (b). Different colors indicate different λ used to generate the beam.

architecture necessary to cohere phased-arrays, greatly reducing the complexity of both the transmit and receive side control architectures while also increasing stability to temperature and environmental variations. Finally, we can emit multiple beams from the device (e.g. exciting all ports simultaneously) without any penalties in beam quality. Note that the size of the system can still be scaled by tiling several lens-based devices in-plane, albeit with some trade-offs.

The beam steering PICs were fabricated on 200 mm wafers in MIT Lincoln Laboratory's (MIT-LL's) 90 nm CMOS capable Microelectronics Laboratory using MIT-LL's SiN PIC platform. The 200 nm tall strip waveguides were fabricated from low pressure chemical vapor deposition (LPCVD) amorphous SiN deposited on top of a smoothed bottom oxide layer. Amorphous silicon gratings were deposited directly on top of the SiN layer, and a top oxide cladding was deposited. A range of PICs were fabricated including devices with 4 to 128 ports, both with and without switching matrices and with and without grating couplers.

As a proof of concept, we measure a 16 port device with a SiN slab=197 nm, a-Si=24.5 nm, and grating pitch Λ=714 nm. Far-field measurements are shown in Fig. 3. The azimuthal angle range is ϕ_{range}=38.8° from ϕ=(21.0° to -17.8°) with a mean angle step increment of $\overline{\Delta\phi}$=2.58° via port switching. The polar angle range is θ_{range}=12.0° from θ=(22.6° to 34.6°) with a mean angle step increment of $\overline{\Delta\theta}$=0.12°/nm via λ tuning from 1500 nm to 1600 nm.

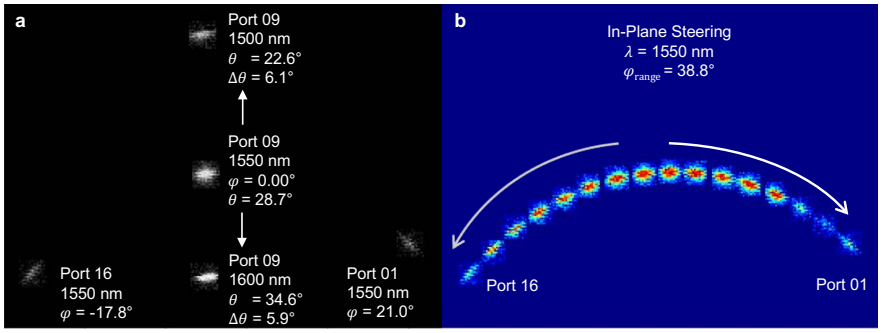

Fig. 3: (a) Experimental far-field measurements of five distinct beams emitted from the device. An IR camera was used to capture the beams emitted from the grating and reflected off a Lambertian surface and then images were superimposed. Switching λ translates a beam up and down. Switching ports translates the beam right to left. (b) Superposition of sweep in port number (1-16), ϕ_{range}=38.8°. The curved path for the port sweep comes from the elliptical equation.

In conclusion, we have demonstrated the first optical planar-lens-enabled beam steering device. It has a range of 38.8°×12.0°. Further theoretical analysis as well as experimental results from devices with larger numbers of ports and switch matrices will be presented at the conference. This work was sponsored by the Assistant Secretary of Defense for Research & Engineering under Air Force Contract No. FA8721-05-C-0002. Opinions, interpretations, conclusions and recommendations are those of the authors and are not necessarily endorsed by the United States Government.

References

1. D. N. Hutchison, J. Sun, J. K. Doylend, R. Kumar, J. Heck, W. Kim, C. T. Phare, A. Feshali, and H. Rong, "High-resolution aliasing-free optical beam steering," Optica, OPTICA **3**, 887–890 (2016).
2. C. V. Poulton, A. Yaacobi, D. B. Cole, M. J. Byrd, M. Raval, D. Vermeulen, and M. R. Watts, "Coherent solid-state LIDAR with silicon photonic optical phased arrays," Opt. Lett., OL **42**, 4091–4094 (2017).
3. W. Rotman and R. Turner, "Wide-angle microwave lens for line source applications," IEEE Transactions on Antennas and Propagation **11**, 623–632 (1963).